PCCP

ROYAL SOCIETY OF CHEMISTRY

PAPER

View Article Online
View Journal | View Issue

Cite this: *Phys. Chem. Chem. Phys.*, 2020, **22**, 6468

Theoretical study on thermal curing mechanism of arylethynyl-containing resins†

Zuowei Chen, Liquan Wang,* Jiaping Lin* and Lei Du

Received 22nd December 2019,
Accepted 2nd March 2020

DOI: 10.1039/c9cp06892a

rsc.li/pccp

Arylethynyl reactive groups have been widely used in high-temperature polymers, and therefore, understanding their curing mechanism is of great importance for academic research and engineering applications. However, no consensus has been achieved on the actual curing mechanism of arylethynyl-containing resins so far. Herein, we present a density functional theory study on the thermal curing mechanism of arylethynyl-containing resins using phenylacetylene and diphenylacetylene as model compounds. It was discovered that the rate-determining step is the dimerization of arylacetylenes into diradical intermediates. The possibilities of the Straus-type intermediates and concerted Diels–Alder cycloaddition between two arylacetylenes can be ruled out. Cyclobutadiene and cyclic allene are the critical intermediates generated by the intramolecular coupling of diradicals. The formation of polyene is preferred by monoradical initiation rather than diradical growth. The overall reaction pathways can well account for the formation of naphthalenic dimers, benzenic trimers, and polyenic chains. The computational results of reactivity for the dimerization of arylacetylenes were finally compared with the existing experimental findings, and an agreement is shown.

Introduction

High-performance polymers produced by thermal curing of the resins containing arylethynyl groups have been widely used in fields such as electronics and aerospace industries due to their excellent thermal stability and mechanical durability.[1–3] The thermal curing of arylethynyl groups is a kind of addition-type reaction, and no volatiles are produced during the reaction, resulting in void-free cross-linked structures. It has been used in a variety of high-temperature polymers, such as polyimides,[4,5] silicon-containing polymers,[6–10] and phenolic resins.[11–13] As the cross-linked structures determine the overall performance of the cured resins, a fundamental understanding of the curing mechanism is of great importance from both academic and engineering viewpoints.

The thermal curing mechanism of arylethynyl-containing resins has been investigated based on oligomers or simplified model compounds in the last few decades. However, the actual curing mechanism is still inconclusive because of the complexity of the curing reaction and the difficulty in characterizing insoluble cured resins. Most of the studies were performed to identify the curing products using solid-state nuclear magnetic resonance (NMR), Fourier-transform infrared spectroscopy (FTIR), *etc.* It was speculated earlier by Landis *et al.* that cyclotrimerization of acetylene units to an aromatic ring is the probable curing reaction.[14] NMR studies by Swanson *et al.* also supported that the major products are aromatic structures in the curing of the acetylene-terminated polyisoimide.[15] However, Sefcik *et al.* found that no more than 30% of the acetylene end-groups undergo cyclotrimerization, through NMR characterization of the structures of acetylene-terminated polyimide resins.[16] Kovar *et al.* proposed that Glaser and Straus coupling products might be generated in the first stage, and the cross-links are further formed through rearrangement, aromatization, and Diels–Alder reaction.[17] In contrast, Gandon *et al.* found that the linear dimers, *i.e.*, the Straus- and Glaser-type compounds, are not the intermediates of thermal polymerization of arylacetylenes by kinetic analysis.[18]

Some other works indicate that the polyenic chains are the major products in the curing of arylethynyl-containing resins. For example, Koening *et al.* found that *trans* conjugated polyenic chains are predominantly formed during the curing of acetylene-terminated sulfone resins using FTIR.[19] A number of works have been reported for the curing reaction of phenylethynyl-terminated polyimides (PETI) studied using NMR. Fang *et al.* found that the major products in the curing of PETI-5 are polyene structures.[20] Furthermore, Roberts *et al.* found that a decrease in the molecular weight of PETI oligomers can result in a higher percentage of polyenes due to the higher concentration of reactive end groups.[21] Gandon *et al.* analyzed the products

Shanghai Key Laboratory of Advanced Polymeric Materials, Key Laboratory for Ultrafine Materials of Ministry of Education, School of Materials Science and Engineering, East China University of Science and Technology, Shanghai 200237, China. E-mail: lq_wang@ecust.edu.cn, jlin@ecust.edu.cn

† Electronic supplementary information (ESI) available. See DOI: 10.1039/c9cp06892a

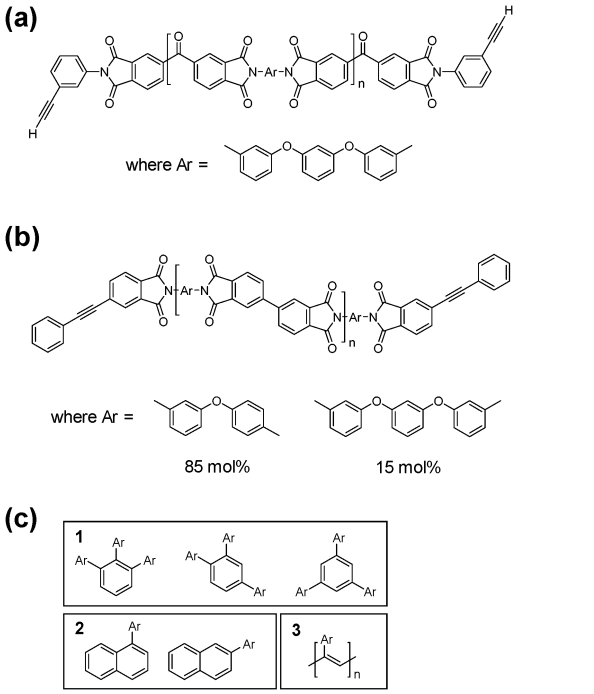

Scheme 1 Representative arylacetylene-containing oligomers: (a) acetylene-terminated imide (ATI) oligomers,[15] (b) phenylethynyl-terminated imide (PETI) oligomers.[20] (c) Possible cross-linked structures: benzenic trimers (1), naphthalenic dimers (2), and polyenic chains (3).

for the thermal polymerization of 4-(hexyloxy)phenylacetylene using chromatography, spectroscopy, and spectrometry techniques.[22] The results indicated that the major products are polyenic chains, and the rest are naphthalenic dimers and benzenic trimers. They suggested a bimolecular initiation mechanism generating diradicals to explain the experimental results.[23] The diradical mechanism was also proposed by Pickard *et al.* in a previously published study.[24]

Despite a lot of experimental studies, no consensus has been reached on the curing mechanism of arylethynyl-containing resins. The experiments showed that the specific proportion of curing products depends on many factors, including the backbone structures and the density of reactive groups, and therefore, the existing experimental findings of curing products vary in different research studies, which could be naphthalenic dimers, benzenic trimers, and polyenic chains (see Scheme 1c). Various mechanisms, such as cyclotrimerization, Diels–Alder reaction, Glaser- or Straus-type couplings, and free radical polymerization, were proposed to explain the formation of the corresponding curing products. Theoretical calculations, which provide fundamental molecular-level information, can be used to study the curing mechanism. Among them, quantum chemical calculations were demonstrated to be an efficient theoretical approach to reveal such complex curing mechanisms.[25,26] However, to our knowledge, there is no comprehensive theoretical study on the curing mechanism of the arylethynyl-containing resins so far.

The purpose of this work is to unveil the mechanism behind the curing of arylethynyl-containing resins and explain the formation of corresponding cross-linked structures by quantum chemical calculations. The potential energy surfaces of the possible reaction pathways, which can enable the establishment of an accurate kinetic model for the curing process, were first explored for both phenylacetylene and diphenylacetylene. Then, the reactivity for the dimerization of arylacetylenes was examined systematically. We finally compared the computational results with the existing experimental observations, and an agreement was found. The work unified the long-standing inconclusive curing mechanism of arylethynyl-containing resins which can guide the further development of new high-temperature polymers.

Computational methodology

All calculations were implemented using the Gaussian 09 program package.[27] Molecular structures in the gas phase were optimized using (U)M06-2X/6-311G(d,p).[28,29] The M06-2X functional was chosen because it was shown to exhibit a good agreement with the experiment for organic structures.[30] Electronic energies were calculated using (U)B3LYP/6-311G(d,p)[31] with a D3 dispersion correction[32] damped according to the scheme of Becke and Johnson.[33] The UB3LYP functional is good at deriving the activation barriers for the dimerization of phenylacetylenes.[34] This combination of methods, denoted as (U)B3LYP-D3BJ/6-311G(d,p)//(U)M06-2X/6-311G(d,p), was successfully applied to the study of the intramolecular hexadehydro-Diels–Alder reaction.[35] HOMO–LUMO mixing for the initial guess was used for open-shell singlet calculations of diradicals. Normal mode analysis was performed to verify whether each optimized structure is a minimum or a transition state. We calculated the intrinsic reaction coordinate (IRC)[36,37] to confirm the connection from each transition state to the corresponding reactants or products.

Since the curing reactions of acetylene-terminated and phenylethynyl-terminated oligomers were generally carried out at temperatures of *ca.* 250 and 350 °C,[2] respectively, all thermal dynamic contributions were computed at 300 °C. Scaling factor of frequencies is 0.946.[38] ΔG and ΔH are the calculated relative free energies and relative enthalpies, respectively, including total electronic energies and thermal contributions. ΔE_0 is zero-point energy (ZPE) corrected relative electronic energies in the gas phase. Unless otherwise specified, all discussed energies refer to ΔG values.

The classical transition state theory (TST) was used to calculate the rate constants $k(T)$ in the gas phase. The rate equation is given by

$$k(T) = \frac{k_B T}{h}\left(\frac{RT}{P^\circ}\right)^{\Delta n} e^{-\frac{\Delta G^\ddagger}{RT}} \quad (1)$$

Here, k_B is the Boltzmann constant, h is the Planck constant, R is the ideal gas constant, and P° is the standard pressure (10^5 Pa). $\Delta G^\ddagger$ represents the standard molar Gibbs free energy of activation for the considered reaction. Δn = 1 or 0 for bimolecular or unimolecular reactions, respectively.

Results and discussion

Considering the computational efficiency, we first chose phenylacetylene, the simplest representative of arylacetylenes, as the compound to model the acetylene-terminated oligomers (Scheme 1a). Note that phenylethynyl is one of the most widely used reactive groups in thermosets, and its cured materials can exhibit an attractive combination of properties. Since the ethynyl groups in phenylethynyl-terminated or -containing oligomers usually bind to aryl groups at both ends, we used diphenylacetylene to model the phenylethynyl-terminated oligomers (Scheme 1b) as a comparison.

We organize the Results and discussion section as follows. First, the favored pathways for the model reaction of phenylacetylene are elucidated. The other competitive but unfavorable pathways are also discussed. Next, the model reaction of diphenylacetylene is compared with that of phenylacetylene to explain the influence of the additional phenyl substituent on the curing reaction. Finally, the reactivity of arylacetylenes in the rate-determining step was examined. In particular, a comparison of the computational results with the existing experimental findings was made to verify the unveiled mechanism.

1. Curing mechanism of acetylene-terminated oligomers using phenylacetylene as the model compound

Overview of the favored reaction pathways of phenylacetylene. The reaction pathways are summarized in Scheme 2, which shows how various cross-linked structures, including naphthalenic dimers, benzenic trimers, and polyenic chains, are formed. Fig. 1 shows the computed energy surfaces for these processes. Structures of transition states in these pathways are given in Fig. 2. DFT calculations show that the curing reaction starts with the dimerization of phenylacetylene **M** to diradical intermediate **INT1**. The diradical intermediate **INT1** could then react with a third molecule of phenylacetylene in *trans* conformation to give a diradical trimer **RAD3,** which can further undergo diradical growth to form polyene products. In another competitive pathway, the diradical intermediate **INT1** could produce strained cyclic allene **INT2** and cyclobutadiene **INT3** *via* an intramolecular coupling.

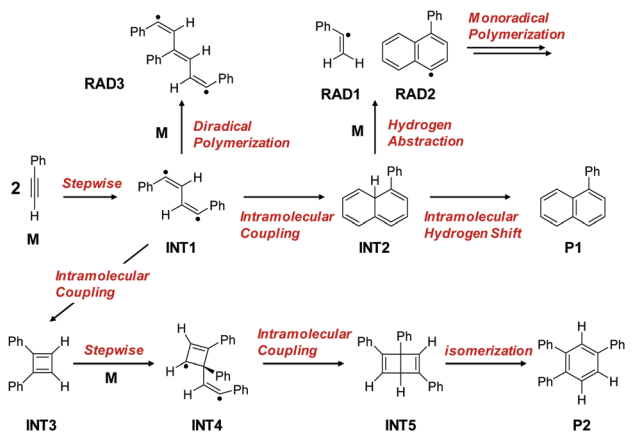

Scheme 2 Curing mechanism of arylethynyl-containing resins based on a phenylacetylene model compound study.

The cyclobutadiene **INT3** reacts with a molecule of phenylacetylene to give diradical intermediate **INT4**, which undergoes ring closure to yield Dewar benzene **INT5**. Isomerization transforms the Dewar benzene **INT5** to the corresponding benzene derivative **P2**.

Notably, how the thermal cyclotrimerization of acetylene units occurs to form different substituted benzenes has been theoretically investigated.[39,40] However, the competition between the cyclotrimerization and other curing reactions in the phenylacetylene model study has not been thoroughly explored, because the phenylacetylene could perform a more complex reaction as discussed later. The strained cyclic allene **INT2** could be rapidly rearranged to naphthalene *via* an intramolecular hydrogen atom shift. This process is the so-called dehydro-Diels–Alder (DDA) reaction.[41,42] The last pathway is that the third molecule of phenylacetylene abstracts a hydrogen atom from **INT2** to generate monoradical initiators **RAD1** and **RAD2** that could initiate chain polymerization to form polyene structures. This process is similar to the self-initiated thermal polymerization of styrene.[43]

Concerted and stepwise mechanisms of phenylacetylene dimerization. The first step of the curing reaction corresponds to the formation of the tail–tail diradical **INT1** (Fig. 1), which is a stepwise pathway to give Diels–Alder adduct **INT2**. In this step, the activation energy is 20.0 kcal mol^{-1}, and the activation free energy is 38.9 kcal mol^{-1}. The activation free energy is much higher than the relative electronic energy because of the unfavorable activation entropy in the bimolecular reaction. In the transition structure **TS1**, the forming C–C bond is 1.76 Å (Fig. 2). Theoretically, there are other competitive stepwise pathways to give diradical intermediates similar to **INT1**. Fig. 3 shows the head–tail transition state **TS1–2** and the head–head transition state **TS1–3** for the dimerization of phenylacetylene. The activation free energies of **TS1**, **TS1–2**, and **TS1–3** are 38.9, 49.8, and 59.0 kcal mol^{-1}, respectively, indicating that the pathway through **TS1** is favored.

Two molecules of phenylacetylene could also dimerize to give two possible Diels–Alder adducts directly, which are concerted pathways. RM06-2X calculations show that the transition state **TS1-con1** is not a stationary point on the potential energy surface because the restricted wave function is unstable. It means that unrestricted wave function is better to describe the electronic structures of the highly asynchronous optimized geometries (Fig. 4). In contrast, RM06-2X locates the concerted transition structure **TS1-con2**. The geometry of **TS1-con2** is more synchronous since the formed C–C bonds differ in length by 0.41 Å, which is much lower than that (1.25 Å) through **TS1-con1**. The activation free energy for **TS1-con2** is 60.6 kcal mol^{-1}. The results above imply that the dimerization of phenylacetylene is not a concerted pathway but a stepwise pathway, due to the larger geometrical change required for the concerted pathways. In short, the favored first step is the pathway through **TS1** with an activation free energy of 38.9 kcal mol^{-1}. The rate constant calculated by the TST method is 8.63 × 10^{-1} s^{-1} mol^{-1} L^{-1} at 300 °C.

Intramolecular couplings to form strained cyclic allene and cyclobutadiene. The ring closure from diradical intermediate **INT1** to strained cyclic allene **INT2** or cyclobutadiene **INT3** is not simple and may involve a series of conformational changes. However, the contribution of conformational changes to

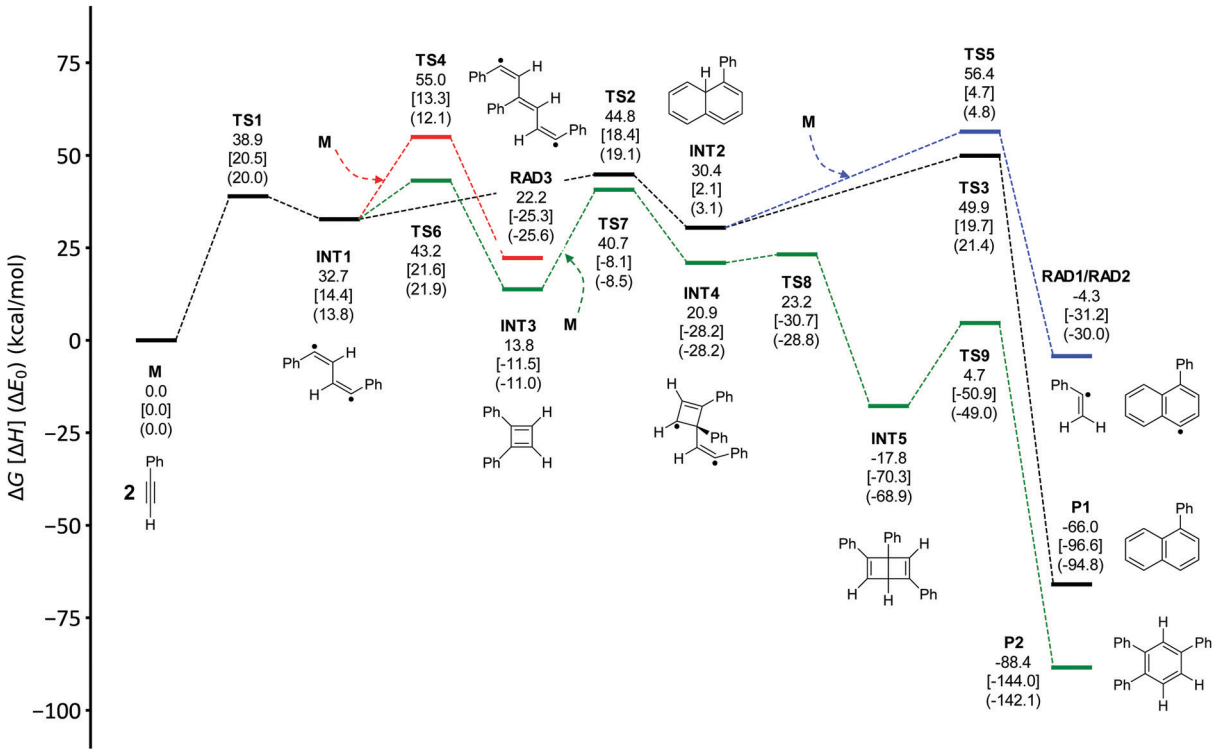

Fig. 1 Energy surfaces of the favored reaction pathways of phenylacetylene. Gibbs free energies and enthalpies [in brackets] are calculated at 573.15 K in the gas phase. Electronic energies with zero-point energy correction (in parenthesis) are also given.

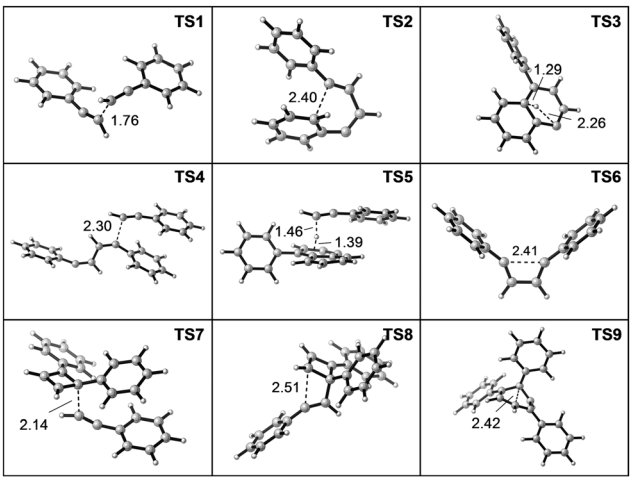

Fig. 2 Transition states in the favored reaction pathways of phenylacetylene. Bond lengths are given in Å.

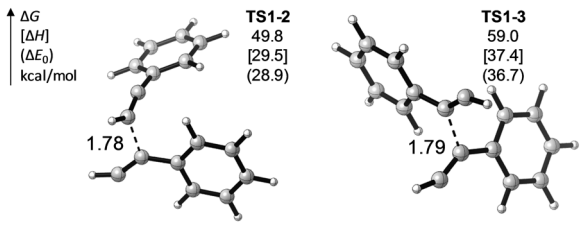

Fig. 3 The other two competitive transition states for the dimerization of phenylacetylene. The energies of the transition states are relative to the energies of two phenylacetylene molecules. Bond lengths are given in Å.

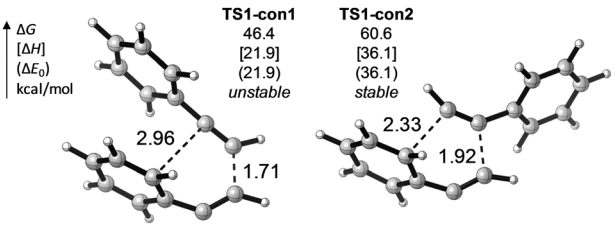

Fig. 4 Transition states for the concerted Diels–Alder cycloaddition of phenylacetylene to form cyclic allene directly. The energies of the transition states are relative to the energies of two phenylacetylene molecules. Bond lengths are given in Å.

activation energies could be tiny. Therefore, we assumed that the **INT1** is the reactant and neglected the conformation changes. The calculations indicate that the **INT1** undergoes fast ring closures to form strained **INT2** and **INT3**. The activation free energies for **TS2** (transition state for forming **INT2**) and **TS6** (transition state for forming **INT3**) are 12.1 and 10.5 kcal mol^{-1}, respectively. In **TS6**, the forming C–C bond is 2.41 Å long, which is very similar to the length (2.40 Å) of the forming C–C bond in **TS2**.

Provided that only the energetic aspect of the competitive reaction is considered, the formation of **INT2** is more favored than that of **INT3** since the activation energies of **TS2** and **TS6** are 5.3 and 8.1 kcal mol^{-1}, respectively. The higher activation free energy of **TS2** may be ascribed to the unfavorable activation entropy arising from the more ordered geometry. In other

words, the **INT1** can only react *via* intramolecular coupling to give cyclic allene **INT2** at a relatively lower temperature. Note that the competitive reaction significantly influences the final products, which can be either the naphthalenic dimers or benzenic trimers. The TST calculations based on the difference in activation free energies indicate that the intramolecular coupling to **INT3** is about four times faster than that of **INT2** at 300 °C. The rate constants for the formation of **INT2** and **INT3** are 2.71×10^8 and 1.13×10^9 s^{-1}, respectively, both of which are incredibly high. The results above suggest that the benzenic trimers are more preferred than the naphthalenic dimers among the final curing structures based on our phenylacetylene model study.

Possibility of the Straus coupling product. Kovar *et al.* proposed that the enynes and diynes resulting from Straus and Glaser couplings, respectively, might be the intermediates of the curing reaction, in order to explain the formation of the products such as naphthalenic dimers and benzenic trimers.[17] However, it has been evidenced that the linear dimers are not the intermediates of the curing reaction based on the model compound study.[18] According to our DFT calculations, it was found that the diradical intermediate **INT1** could generate enyne, namely, Straus-type product, by an intramolecular hydrogen shift (shown in Scheme 3). The transition structure **TS-St** is shown in Fig. 5. The activation free energy of the formation of enyne is 27.0 kcal mol^{-1}, which is much higher than the activation free energies (12.1 and 10.5 kcal mol^{-1}) of the intramolecular coupling reactions. Therefore, we can rule out the formation of Straus-type products due to unfavorable kinetics despite there being a reaction pathway.

Formation of benzenic trimer. The diphenylcyclobutadiene **INT3** can react with a phenylacetylene molecule to generate Dewar benzene **INT5**, which then isomerizes into benzenic trimer **P2** (see Scheme 2). These reactions have been thoroughly investigated in thermal cyclotrimerization of substituted acetylene using quantum chemistry methods.[39,40] In this study, we attempted to elucidate the reaction pathway with density functional calculations to understand the overall process of the curing reaction. The favored pathway shown in Fig. 1 indicates that the reaction of **INT3** to **INT4** *via* transition structure **TS7** requires an activation free energy of 26.9 kcal mol^{-1} and follows a diradical mechanism. Then **INT4** undergoes ring closure to yield Dewar benzene **INT5** with an activation free energy of 2.3 kcal mol^{-1}. Finally, **INT5** isomerizes to **P2** with an activation free energy of 22.5 kcal mol^{-1}. These activation free energies are lower than that (38.9 kcal mol^{-1}) for the dimerization of phenylacetylene, suggesting that **INT3** can rapidly evolve into **P2**. The activation energies of the other competitive pathways for the evolution of diphenylcyclobutadiene into benzene derivatives are presented in Fig. S1 and S2 of the ESI.†

Monoradical and diradical initiated polymerizations. Radical polymerization of ethynyl groups into polyene is a critical step in the curing reaction of oligomers containing arylethynyl groups. Two processes could potentially initiate radical polymerization. One is that the diradical intermediate **INT1** reacts with another phenylacetylene molecule to initiate diradical polymerization, as shown in Scheme 2. The other diradical growth pathways can be seen in Fig. S3 of the ESI.† The activation free energy is 22.3 kcal mol^{-1}, which is higher than that (10.5 kcal mol^{-1}) of the intramolecular coupling of **INT1** to cyclobutadiene **INT3**. Intramolecular coupling to **INT3** occurs over 10^2 times faster than diradical growth, as calculated using the TST method.

It was noted that short diradical polymer chains are more likely to undergo intramolecular termination than grow to a high-molecular-weight polymer in polymerization with diradical initiators.[44] Moreover, the DFT calculations on self-initiated thermal polymerization of styrene suggest that the diradical growth is disfavored because the self-termination of the 1,4-diradical occurs over 10^{11} times faster than the diradical growth predicted by the TST method.[43] We can see that the difference in reaction rates between intramolecular coupling and diradical growth in phenylacetylene polymerization is much less than that in styrene polymerization. However, the intramolecular coupling of **INT1** is still more favored than the diradical growth, because the diradical growth to **RAD3** is a bimolecular reaction with unfavorable activation entropies.

Nevertheless, the reaction energy surfaces show that the activation energy of the diradical growth is at least 7 kcal mol^{-1} lower than that of the intramolecular coupling. It means that the diradical growth is more favored than the intramolecular coupling if only the energetic aspects of the competitive reactions are taken into account. The higher activation energy for the intramolecular coupling is probably due to the more substantial activation strain energy. The results indicate that diradical growth could probably occur at relatively lower temperatures and/or higher concentrations under which the bimolecular diradical growth is favored over the unimolecular cyclization.

Another consideration is that the strained cyclic allene **INT2** could evolve into aromatic products by an intramolecular hydrogen shift or by intermolecular hydrogen abstraction. Phenylacetylene abstracts a hydrogen atom from cyclic allene **INT2** to generate styryl radical **RAD1** and naphthyl radical **RAD2**, both of which

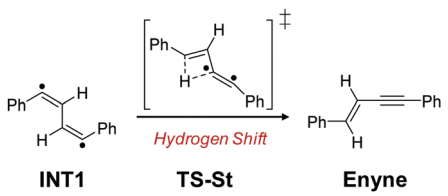

Scheme 3 Intramolecular hydrogen shift of diradical **INT1** into **Enyne**.

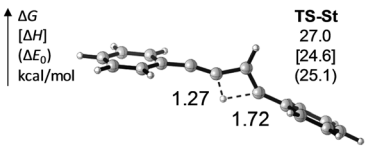

Fig. 5 The transition state for the intramolecular hydrogen shift of diradical **INT1** into **Enyne**. The energies of **TS-St** are relative to the energies of **INT1**. Bond lengths are given in Å.

are capable of initiating chain polymerization. This process is similar to the Mayo mechanism for the spontaneous thermal polymerization of styrene.[45,46] The computational results show that the restricted wave function of **TS3** optimized by RM06-2X is stable, while the UB3LYP calculation indicates that it is a singlet diradical for the same structure. The $\langle S^2 \rangle$ value computed by UB3LYP is 0.0134. The activation free energy of the hydrogen abstraction is 26.0 kcal mol^{-1}, which is higher than the activation free energy (19.5 kcal mol^{-1}) of the intramolecular hydrogen shift. The activation energy of the hydrogen abstraction is 1.7 kcal mol^{-1} significantly lower than that of the intramolecular hydrogen shift, suggesting that the monoradical initiator could be produced enough at relatively lower temperatures and/or higher concentrations. Those energetically favored effects for the bimolecular reaction have also been discussed in the competitive reactions of enediyne dimerization *versus* Bergman cyclization.[47]

In addition, the difference in activation free energy between the intermolecular hydrogen abstraction and intramolecular hydrogen shift is 6.5 kcal mol^{-1}, which is much lower than that (11.8 kcal mol^{-1}) between the diradical growth and intramolecular coupling. Finally, the rates at which the diradical **INT1** produces cyclic allene **INT2** and cyclobutadiene **INT3** are slightly different, implying that the formation of polyene is preferred by monoradical initiation instead of diradical growth. This result is consistent with the previous experiment that the high polymer produced in a diradical-initiated system primarily results from monoradicals formed by a chain transfer reaction.[44]

2. Curing mechanism of phenylethynyl-terminated oligomers using diphenylacetylene as the model compound

Fig. 6 shows the free energy surfaces of the favored reaction pathways for diphenylacetylene. Corresponding transition structures are presented in Fig. 7. The other competitive but unfavorable pathways are presented in Fig. S4 and S5 of the ESI.† The computed energy surfaces of diphenylacetylene are very similar to those of phenylacetylene. The formation of cyclic allene **INT2-Ph** or cyclobutadiene **INT3-Ph** is stepwise. These processes involve the diradical intermediate **INT1-Ph** with an activation free energy of 45.4 kcal mol^{-1} at 300 °C, which is 6.5 kcal mol^{-1} higher than that for the dimerization of phenylacetylene. The rate constant calculated by the TST method at 300 °C is 2.88×10^{-3} s^{-1} mol^{-1} L^{-1}, which is two orders of magnitude lower than that of the phenylacetylene dimerization. This implies that a higher temperature is required to cure the diphenylacetylene. As previously mentioned, diphenylacetylene is simplified from phenylethynyl-terminated oligomers. This can explain the reason that the curing temperature of phenylethynyl-terminated oligomers is about 100 °C higher than that of acetylene-terminated oligomers and that the phenylacetylene-terminated oligomers have a broader process window.[2]

The transition state for concerted cycloaddition of diphenylacetylene is presented in Fig. 8. As expected, the restricted wave function is proved to be unstable, and the activation free energy of the concerted route is 55.1 kcal mol^{-1}, which is higher than that of the stepwise route. The subsequent intramolecular couplings of **INT1-Ph** to cyclic allene **INT2-Ph** and cyclobutadiene **INT3-Ph**

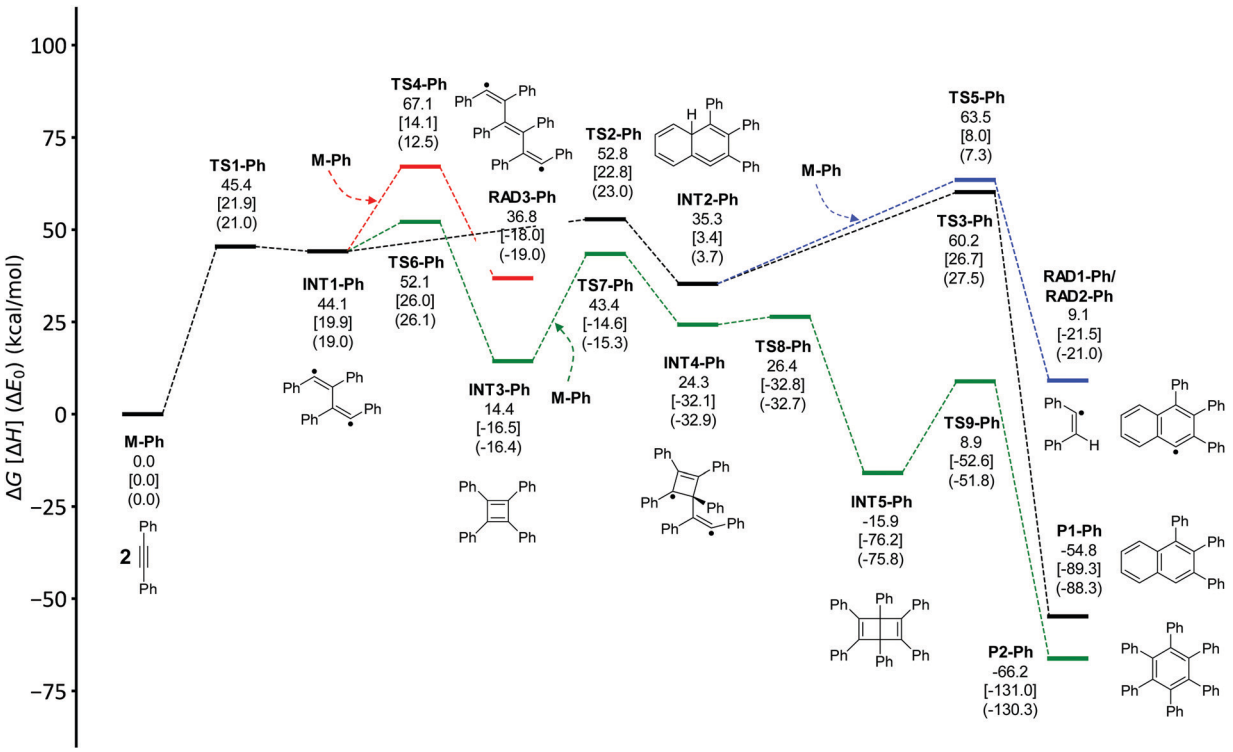

Fig. 6 Energy surfaces of the favored reaction pathways of diphenylacetylene.

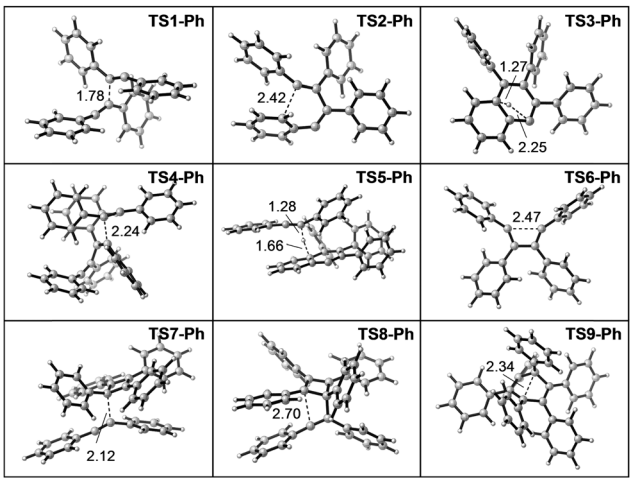

Fig. 7 Transition states in the favored reaction pathways of diphenylacetylene. Bond lengths are given in Å.

require activation free energies of 8.7 and 8.0 kcal mol^{-1}, respectively. The difference in the activation free energies between **TS2-Ph** and **TS6-Ph** is only 0.7 kcal mol^{-1}, which is slightly lower than that of 1.6 kcal mol^{-1} between **TS2** and **TS6**. It indicates that the influences of the phenyl group and the hydrogen atom, which are attached to the new bonding carbon atoms, are less marked on the competitive intramolecular couplings.

The cyclobutadiene **INT3-Ph** can react with a diphenylacetylene molecule to yield the diradical intermediate **INT4-Ph** with an activation free energy of 29.0 kcal mol^{-1}. Then **INT4-Ph** undergoes ring closure to yield the Dewar benzene **INT5-Ph** with an activation free energy of 2.1 kcal mol^{-1}. The **INT5-Ph** further isomerizes into **P2-Ph** with an activation free energy of 24.8 kcal mol^{-1}. Besides, the activation free energy for the diradical growth of **INT1-Ph** with another phenylacetylene molecule is 23.0 kcal mol^{-1}, which is 15.0 kcal mol^{-1} higher than that for intramolecular coupling of **INT1-Ph** to tetraphenylcyclobutadiene **INT3-Ph**. The difference in activation free energies suggests that the formation of **INT3-Ph** occurs over 10^4 times faster than diradical growth. It indicates that diradical initiation is more disfavored in diphenylacetylene polymerization than in phenylacetylene polymerization as described above. If only the energetic aspect of the competitive reaction is taken into account, the activation energy $\Delta E_0^{\ddagger}$ is −6.5 kcal mol^{-1}, which is lower than that (−1.7 kcal mol^{-1}) of

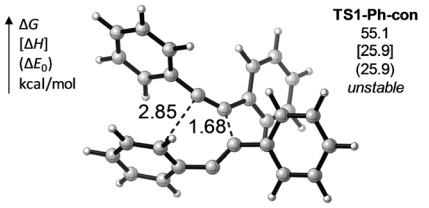

Fig. 8 The transition state for the concerted Diels–Alder cycloaddition of diphenylacetylene to form cyclic allene directly. The energies of the transition state are relative to the energies of two diphenylacetylene molecules. Bond lengths are given in Å.

diradical initiation in phenylacetylene polymerization. Both the activation energies are negative, probably due to the fact that the interaction in the transition state increases with respect to the separate reactant molecules. Therefore, the phenyl groups attached to the new bonding carbon atoms reduce the rate of diradical growth. This is because transition structure **TS4-Ph** suffers from additional interaction effects, which results in a more ordered geometry and a lower entropy, but is not due to the electronic effect. The activation free energy for abstracting a hydrogen atom from cyclic allene **INT2-Ph** to a diphenylacetylene molecule is 28.2 kcal mol^{-1}, which is only 3.3 kcal mol^{-1} higher than that (24.9 kcal mol^{-1}) of the intramolecular hydrogen shift of **INT2-Ph** to produce the naphthalenic product **P1-Ph**.

The computational results above indicate that the proportion of monoradical initiation in diphenylacetylene polymerization is larger than that in phenylacetylene polymerization. In addition, the rates for both the intramolecular and intermolecular hydrogen transfer in diphenylacetylene polymerization decreases as compared with those in phenylacetylene polymerization. The reason for this may be that the additional phenyl groups increase the stability of **INT2-Ph** due to the conjugation effect between phenyl and allene.

3. Dimerization of arylacetylenes and comparison with experimental results

The curing temperature of resins depends on many factors such as molecular diffusivity, the density of reactive groups, and the location of groups on the molecule. Herein, we focus on the reactivity of arylacetylene, which is essential to the molecular design of new polymers containing arylethynyl groups. Many efforts have been made to explore the influences of molecular structures on curing temperature. However, the experimental overall activation energy, which is usually estimated from DSC analysis, involves many factors such as diffusion of reactants that are incapable of being studied using DFT methods. Recently, high-level quantum chemical calculations revealed that electron-withdrawing groups attached to the reacting centers and the substituents with high donor abilities bound to the aryl systems reduce the activation barriers for the dimerization of arylacetylenes.[34,48] The electronic influence of the substituents on the reactivity of arylacetylenes was analysed in detail. In this subsection, several arylacetylene structures commonly used in high-temperature polymers were chosen, and comparisons between our computed results with the existing experimental studies were made. The aim was to verify the reaction mechanism by reproducing the reactivity trends of the model compounds (**1–8** as shown in Scheme 4).

We also analyzed the activation barriers using the distortion/interaction model.[49,50] The activation barrier $\Delta E^{\ddagger}$ for a bimolecular reaction can be decomposed into the distortion energy $\Delta E_d^{\ddagger}$ and interaction energy $\Delta E_i^{\ddagger}$. The activation barrier can then be represented as $\Delta E^{\ddagger} = \Delta E_d^{\ddagger} + \Delta E_i^{\ddagger}$, where E is the total electronic energy without zero-point energy correction. The distortion energy $\Delta E_d^{\ddagger}$ is the energy required to distort the molecules. The interaction energy $\Delta E_i^{\ddagger}$ is related to the bonding capabilities and interaction between the reactants, which is usually negative. All of these computed results are shown in Table 1.

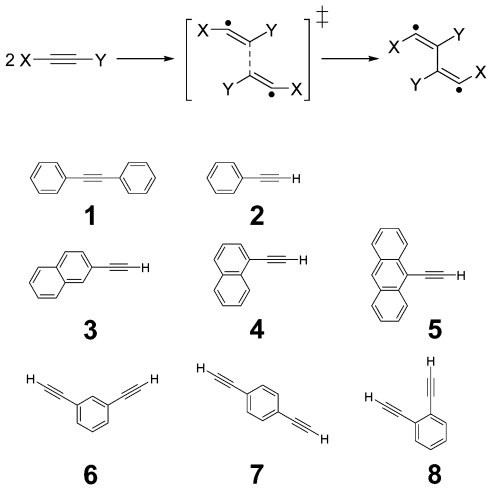

Scheme 4 Dimerization of arylacetylenes **1–8** to diradicals.

Table 1 Activation barriers ($\Delta E^{\ddagger}$), distortion energies ($\Delta E_{d}^{\ddagger}$), and interaction energies ($\Delta E_{i}^{\ddagger}$) in kcal mol^{-1} for the dimerization of corresponding arylacetylenes. The $\Delta E_{d}^{\ddagger}$ and $\Delta E_{i}^{\ddagger}$ are computed using B3LYP-D3BJ/6-311G(d,p)

Compound	$\Delta E^{\ddagger}$ [a]	$\Delta E^{\ddagger}$ [b]	$\Delta E_{d}^{\ddagger}$	$\Delta E_{i}^{\ddagger}$
1	22.3	31.7	28.3	−6.0
2	20.9	29.8	20.9	0.0
3	20.2	29.1	21.2	−1.0
4	19.0	28.0	20.2	−1.2
5	15.2	24.2	16.8	−1.6
6	20.8	29.6	21.2	−0.4
7	19.0	28.1	20.0	−1.0
8	18.5	27.4	19.8	−1.3

[a] (U)B3LYP-D3BJ/6-311G(d,p)//(U)M06-2X/6-311G(d,p). [b] (U)M06-2X/6-311G(d,p).

From the free energy surfaces shown in Fig. 1 and 6, we can see that the dimerization of two arylacetylenes is the rate-determining step. The calculated rate constants are 8.63×10^{-1} and 2.88×10^{-3} s^{-1} mol^{-1} L^{-1} for phenylacetylene and diphenylacetylene, respectively, at 300 °C. Considering the effect of diffusion in the actual system, both of them are within a reasonable range. The distortion energy for the dimerization of diphenylacetylene is 28.3 kcal mol^{-1}, and the corresponding interaction energy is −6.0 kcal mol^{-1} (Table 1, compound **1**). For comparison, the distortion and interaction energies are 20.9 and 0.0 kcal mol^{-1}, respectively, for the dimerization of phenylacetylene (Table 1, compound **2**). It implies that the extra bends of two C–C–C angles for dimerization of diphenylacetylene, which reduce the conjugative stabilization between phenyl and ethynyl, are the principal contributors to the higher activation barrier.

Wright *et al.* investigated the substituent effects of the ethynyl on the thermal curing kinetics and revealed that the new arylethynyl endcaps such as naphthyl-ethynyl and anthracenyl-ethynyl could accelerate the thermal curing rate.[51,52] For simplicity, we examined the dimerization of 2-naphthylacetylene, 1-naphthylacetylene, and 9-anthracenylacetylene (compounds **3–5** in Scheme 4). The computed results indicate that the activation barriers $\Delta E^{\ddagger}$ decrease in the sequence of phenyl > 2-naphthyl > 1-naphthyl > 9-anthracenyl (see Table 1, compounds **2–5**), which is consistent with the experimental results. Structures of the transition states are shown in Fig. S6 of the ESI.† Besides, the interaction and distortion energies of transition structures follow the same sequence, which could be ascribed to the increased conjugate stabilization of diradical centers. Notably, the lower activation barrier of compound **5** (9-anthracenyl) mainly comes from the higher conjugate stabilization of diradical centers, since the distortion energy (16.8 kcal mol^{-1}) is much lower than that of compounds **2–4**. This distortion-acceleration effect also exists in the stepwise hexadehydro-Diels–Alder (HDDA) reactions accelerated by alkynyl substituents.[53]

Sastri *et al.* investigated the effects of the relative positions of the acetylenic substituents on the aromatic ring and proposed that the additional resonance stabilization of radicals could reduce the activation energy.[54] Their experimental results suggest that the activation energies of the 1,2- and 1,4-disubstituted acetylenic compounds are significantly lower than that of the 1,3-disubstituted acetylenic compounds. Our computed results indicate that the activation barriers $\Delta E^{\ddagger}$ decrease in the sequence of 1,3- > 1,4- > 1,2-disubstituted acetylenic compounds (see Table 1, compounds **6–8**). Structures of the transition states are shown in Fig. S6 of the ESI.† This is in good agreement with the experimental results. The distortion/interaction analysis shows that the decreasing activation barriers come from both decreasing distortion and interaction energies.

A remaining consideration is the activation barriers obtained by (U)B3LYP-D3BJ and (U)M06-2X. The calculations using both methods show the same variation tendency of activation barriers (shown in Table 1). However, (U)M06-2X predicts the activation barriers to be over an average of 9 kcal mol^{-1} than (U)B3LYP-D3BJ. Since both methods are based on a single reference configuration and cannot describe the degenerated correlation effects, careful calibration against both experimental results and multireference approaches is necessary. It has been found that UM06-2X overestimates the energies of the diradical transition states.[35,55] Many studies for diradicals indicate that the activation barriers derived by the UB3LYP functional are in good quantitative agreement with the experimental results.[34,35,48] Therefore, the method used in this study, namely (U)B3LYP-D3BJ/6-311G(d,p)//(U)M06-2X/6-311G(d,p), is reasonable for the investigated system. The comparison of computed results with the existing experiments confirmed the proposed curing mechanism.

Summarizing the above results, the detailed curing mechanism of the arylethynyl groups was elucidated, which can explain the formation of cross-linked structures observed in the existing experiments. We want to emphasize that the fundamental understanding of this curing mechanism is of value in developing the resins with high thermal stability and excellent mechanical properties. The high thermal stability of the cured resins mainly comes from the aromatic cross-linked structures. Those aromatic structures are rigid, and therefore, the resins based on these structures usually have low toughness. In contrast, polyene structures derived from chain extension

render the cured resin reasonable toughness but relatively low thermal stability.[2,56] The computational results show that the intramolecular coupling to form cyclic allene or cyclobutadiene is the critical step in the formation of aromatic structures. Additionally, the diradical and monoradical intermediates could both initiate the polymerization of arylethynyl groups to form polyenic chains. Our work provides an insight into the favored reaction pathway of thermal curing of arylethynyl-containing resins, which helps tune the final curing products.

On the other hand, the processing of the arylethynyl-containing resins is highly dependent on the curing temperature. In general, the processing window is related to the glass transition temperature (T_g) and the initial curing temperature of the uncured resin.[2,57] An uncured resin with a lower T_g and higher initial curing temperature can be generally processed with a broader processing window. However, a fast curing rate is often required to realize the economy in curing time. Therefore, a low initial curing temperature is needed in some cases. Our study for the dimerization of arylacetylenes provides molecular-level information of this curing reaction and gives a qualitative picture of controlling the curing temperature of arylethynyl-containing resins.

Conclusions

We examined the thermal curing mechanism of the resins containing arylethynyl groups by the DFT study. Two model compounds of phenylacetylene and diphenylacetylene were considered. The major cross-linking pathway includes the dimerization of two arylacetylenes into a diradical intermediate, which then undergoes the intramolecular couplings to strained cyclic allene and cyclobutadiene, followed by the evolution into naphthalenic dimer and benzenic trimer. The dimerization of arylacetylenes into diradical intermediates was found to be the rate-determining step. The Straus-type products were ruled out due to the unfavorable kinetics. The monoradical initiation is more favored than diradical growth for the formation of polyenic chains. The overall reaction mechanism nicely explains the formation of various curing structures, including naphthalenic dimers, benzenic trimers, and polyenic chains. The reactivity trends for the dimerization of arylacetylenes can be well accounted for by the computed activation barriers. The computational results are consistent with the existing experimental findings.

Conflicts of interest

There are no conflicts to declare.

Acknowledgements

This work was supported by the National Natural Science Foundation of China (51833003, 21975073, and 21774032). Support from the Project of Shanghai Municipality (16520721900) and the Fundamental Research Funds for the Central Universities (50321041918013) is also appreciated.

References

1 P. M. Hergenrother, *J. Macromol. Rev. Sci., Rev. Macromol. Chem.*, 1980, **C19**, 1–34.
2 J. W. Connell, J. G. Smith Jr. and P. M. Hergenrother, *J. Macromol. Sci., Rev. Macromol. Chem. Phys.*, 2000, **C40**, 207–230.
3 P. M. Hergenrother, *High Perform. Polym.*, 2003, **15**, 3–45.
4 P. M. Hergenrother, J. W. Connell and J. G. Smith Jr., *Polymer*, 2000, **41**, 5073–5081.
5 C. M. Thompson and P. M. Hergenrother, *Macromolecules*, 2002, **35**, 5835–5839.
6 M. Itoh, K. Inoue, K. Iwata, M. Mitsuzuka and T. Kakigano, *Macromolecules*, 1997, **30**, 694–701.
7 S. Kuroki, K. Okita, T. Kakigano, J. Ishikawa and M. Itoh, *Macromolecules*, 1998, **31**, 2804–2808.
8 F. Wang, J. Zhang, J. Huang, H. Yan, F. Huang and L. Du, *Polym. Bull.*, 2006, **56**, 19–26.
9 Q. Li, Y. Zhou, X. Hang, S. Deng, F. Huang, L. Du and Z. Li, *Eur. Polym. J.*, 2008, **44**, 2538–2544.
10 M. Chu, J. L. Zhu, L. Q. Wang, J. P. Lin, L. Du and C. H. Cai, *Acta. Polym. Sin.*, 2019, **50**, 1–9.
11 C. P. R. Nair, *Prog. Polym. Sci.*, 2004, **29**, 401–498.
12 C. P. R. Nair, R. L. Bindu and K. N. Ninan, *J. Mater. Sci.*, 2001, **36**, 4151–4157.
13 H. J. Kim, Z. Brunovska and H. Ishida, *Polymer*, 1999, **40**, 1815–1822.
14 A. Landis, N. Bilow, R. Boschan, R. Lawrence and T. Aponyi, *Polym. Prepr. (Am. Chem. Soc., Div. Polym. Chem.)*, 1974, **15**, 537–541.
15 S. A. Swanson, W. W. Fleming and D. C. Hofer, *Macromolecules*, 1992, **25**, 582–588.
16 M. D. Sefcik, E. O. Stejskal, R. A. McKay and J. Schaefer, *Macromolecules*, 1979, **12**, 423–425.
17 R. F. Kovar, G. F. L. Ehlers and F. E. Arnold, *J. Polym. Sci., Polym. Chem. Ed.*, 1977, **15**, 1081–1095.
18 S. Gandon, P. Mison and B. Sillion, *Polymer*, 1997, **38**, 1449–1459.
19 J. L. Koenig and C. M. Shields, *J. Polym. Sci., Polym. Phys. Ed.*, 1985, **23**, 845–859.
20 X. Fang, X. Q. Xie, C. D. Simone, M. P. Stevens and D. A. Scola, *Macromolecules*, 2000, **33**, 1671–1681.
21 C. C. Roberts, T. M. Apple and G. E. Wnek, *J. Polym. Sci., Part A: Polym. Chem.*, 2000, **38**, 3486–3497.
22 S. Gandon, P. Mison, M. Bartholin, R. Mercier, B. Sillion, E. Geneve, P. Grenier and M. F. Grenier-Loustalot, *Polymer*, 1997, **38**, 1439–1447.
23 S. Gandon, P. Mison and B. Sillion, *ACS Symp. Ser.*, 1996, **624**, 306–321.
24 J. M. Pickard, E. G. Jones and I. J. Goldfarb, *Macromolecules*, 1979, **12**, 895–902.
25 J. E. Ehlers, N. G. Rondan, L. K. Huynh, H. Pham, M. Marks and T. N. Truong, *Macromolecules*, 2007, **40**, 4370–4377.
26 S. Kunnikuruvan, P. V. Parandekar, O. Prakash, T. K. Tsotsis and N. N. Nair, *Macromolecules*, 2017, **50**, 6081–6087.
27 M. J. Frisch, *et al.*, *Gaussian 09, Revision C.01*, Wallingford, CT, 2010, Full citation can be found in the ESI†.

28 Y. Zhao and D. G. Truhlar, *Theor. Chem. Acc.*, 2008, **120**, 215–241.
29 R. Krishnan, J. S. Binkley, R. Seeger and J. A. Pople, *J. Chem. Phys.*, 1980, **72**, 650–654.
30 Y. Zhao and D. G. Truhlar, *Chem. Phys. Lett.*, 2011, **502**, 1–13.
31 P. J. Stephens, F. J. Devlin, C. F. Chabalowski and M. J. Frisch, *J. Phys. Chem.*, 1994, **98**, 11623–11627.
32 S. Grimme, J. Antony, S. Ehrlich and H. Krieg, *J. Chem. Phys.*, 2010, **132**, 154104.
33 E. R. Johnson and A. D. Becke, *J. Chem. Phys.*, 2006, **124**, 174104.
34 S. Fabig, G. Haberhauer and R. Gleiter, *J. Am. Chem. Soc.*, 2015, **137**, 1833–1843.
35 D. J. Marell, L. R. Furan, B. R. Woods, X. Lei, A. J. Bendelsmith, C. J. Cramer, T. R. Hoye and K. T. Kuwata, *J. Org. Chem.*, 2015, **80**, 11744–11754.
36 K. Fukui, *J. Chem. Phys.*, 1970, **74**, 4161–4163.
37 C. Gonzalez and H. B. Schlegel, *J. Chem. Phys.*, 1990, **94**, 5523–5527.
38 D. O. Kashinski, G. M. Chase, R. G. Nelson, O. E. Di Nallo, A. N. Scales, D. L. VanderLey and E. F. C. Byrd, *J. Phys. Chem. A*, 2017, **121**, 2265–2273.
39 Z. K. Yao and Z. X. Yu, *J. Am. Chem. Soc.*, 2011, **133**, 10864–10877.
40 G. O. Jones and Z. J. Krebs, *Org. Biomol. Chem.*, 2017, **15**, 8326–8333.
41 P. Wessig and G. Müller, *Chem. Rev.*, 2008, **108**, 2051–2063.
42 A. Ajaz, A. Z. Bradley, R. C. Burrell, W. H. Li, K. J. Daoust, L. B. Bovee, K. J. Di Rico and R. P. Johnson, *J. Org. Chem.*, 2011, **76**, 9320–9328.
43 K. S. Khuong, W. H. Jones, W. A. Pryor and K. N. Houk, *J. Am. Chem. Soc.*, 2005, **127**, 1265–1277.
44 J. D. Rule, S. R. Wilson and J. S. Moore, *J. Am. Chem. Soc.*, 2003, **125**, 12992–12993.
45 F. R. Mayo, *J. Am. Chem. Soc.*, 1968, **90**, 1289–1295.
46 Y. K. Chong, E. Rizzardo and D. H. Solomon, *J. Am. Chem. Soc.*, 1983, **105**, 7761–7762.
47 G. Haberhauer, R. Gleiter and S. Fabig, *Org. Lett.*, 2015, **17**, 1425–1428.
48 S. Fabig, A. Janiszewski, M. Floß, M. Kreuzahler and G. Haberhauer, *J. Org. Chem.*, 2018, **83**, 7878–7885.
49 D. H. Ess and K. N. Houk, *J. Am. Chem. Soc.*, 2007, **129**, 10646–10647.
50 D. H. Ess and K. N. Houk, *J. Am. Chem. Soc.*, 2008, **130**, 10187–10198.
51 M. E. Wright, D. A. Schorzman and L. E. Pence, *Macromolecules*, 2000, **33**, 8611–8617.
52 M. E. Wright and D. A. Schorzman, *Macromolecules*, 2001, **34**, 4768–4773.
53 Y. Liang, X. Hong, P. Yu and K. N. Houk, *Org. Lett.*, 2014, **16**, 5702–5705.
54 S. B. Sastri, T. M. Keller, K. M. Jones and J. P. Armistead, *Macromolecules*, 1993, **26**, 6171–6174.
55 N. C. James, J. M. Um, A. B. Padias, H. K. Hall, Jr. and K. N. Houk, *J. Org. Chem.*, 2013, **78**, 6582.
56 C. Liu, X. Zhao, X. Yu, W. Wang, H. Jia, Y. Li, H. Zhou and C. Chen, *Polym. Degrad. Stab.*, 2013, **98**, 230–240.
57 D. Cho and L. T. Drzal, *J. Appl. Polym. Sci.*, 2000, **76**, 190–200.